Sustainable Environment Research

RESEARCH Open Access

Nb_2O_5 monolith as an efficient and reusable catalyst for textile wastewater treatment

Franco David Troncoso[1,2] and Gabriela Marta Tonetto[1,2*]

Abstract

In this work, the degradation of methylene blue (MB) in aqueous solution by a heterogeneous Fenton-like process was studied. Nb_2O_5 supported on an anodized aluminum monolith was used as catalyst. The Nb_2O_5 coating generated during the catalyst synthesis was uniform and porous, with a thickness of 7 μm. Response surface methodology was used to study the relationship between process variables and MB degradation and chemical oxygen demand (COD) reduction. The optimal operating conditions were: initial MB concentration of 45 mg L^{-1}, initial H_2O_2 concentration in the reaction medium of 40 mM, catalyst loading of 7.85 $kg_{Nb_2O_5}$ m^{-3}, and pH 4, reaching a MB degradation of 98% and a COD reduction of 79% at 150 min. The high activity of the Nb_2O_5 monolith catalyst remained constant after 10 catalytic tests.

Keywords: Monolithic catalyst, Niobia, Anodic alumina, Dye, Methylene blue

Introduction

Textile industries are responsible for serious environmental problems due to the large volume of dyestuff wastewater that they generate (200 to 350 m^3 of wastewater per ton of finished product) [1]. Textile wastewaters commonly present high values of pH, biochemical oxygen demand (BOD), chemical oxygen demand (COD), turbidity, and occasionally potential carcinogenic or mutagenic substances [2]. Colored wastewater also reduces the light penetration through the water surface, and consequently the photosynthetic activity of aquatic organisms [3].

Nowadays, conventional technologies applied for textile wastewater treatment are based on coagulation-flocculation processes, activated carbon adsorption and membrane filtration technique. These methods are non-destructive, transferring the organic contaminant to another medium that demands further treatment, thus increasing the processing costs. On the other hand, biological wastewater treatment methods generally have a low efficiency in color removal due to the high resistance of the organic dye compounds to degradation [2].

In this context, advanced oxidation processes (AOP) using heterogeneous catalysts are considered a promising technology for the discoloration of textile wastewater, as they lead to the total mineralization of most organic pollutants without generating solid wastes [4]. In recent years, there has been a growing interest in the application of niobia (Nb_2O_5) for water remediation due to its acid sites properties, good chemical stability, null toxicity and commercial availability [5].

The application of niobium pentoxide nanoparticles for dye photodegradation has been previously studied, exhibiting promising performances [6, 7]. Kumari et al. [8] reported a dyestuff degradation (methylene blue, MB) of between 40 and 70% using Nb_2O_5 nanoparticles as photocatalyst. de Carvalho et al. [6] observed almost 100% MB degradation using niobium pentoxide as photocatalyst after 3 h of sunlight exposure. In contrast, dyes in high concentration limit the light penetration

* Correspondence: gtonetto@plapiqui.edu.ar
[1]Chemical Engineering Department, University National of the South, 8000 Bahía Blanca, Argentina
[2]Pilot Plant of Chemical Engineering, National Council for Scientific and Technological Research, 8000 Bahía Blanca, Argentina

© The Author(s). 2021 **Open Access** This article is licensed under a Creative Commons Attribution 4.0 International License, which permits use, sharing, adaptation, distribution and reproduction in any medium or format, as long as you give appropriate credit to the original author(s) and the source, provide a link to the Creative Commons licence, and indicate if changes were made. The images or other third party material in this article are included in the article's Creative Commons licence, unless indicated otherwise in a credit line to the material. If material is not included in the article's Creative Commons licence and your intended use is not permitted by statutory regulation or exceeds the permitted use, you will need to obtain permission directly from the copyright holder. To view a copy of this licence, visit http://creativecommons.org/licenses/by/4.0/.

into the solution, increasing the light scattering effect, and decreasing the process efficiency [9].

Niobium pentoxide is also a suitable catalyst for oxidation reactions using hydrogen peroxide (H_2O_2) as oxidant [10]. Ziolek et al. [11] reported that Nb_2O_5 contacted with hydrogen peroxide exhibited high ability to form radical peroxo species, generating active oxygen for the alcohol oxidation. On the other hand, textile wastewater treatments using Nb_2O_5 catalyst, in non-photocatalytic systems, have been scarcely reported [12]. Oliveira et al. [13] observed that the presence of hydrogen peroxide enhances the generation of hydroxyl radicals, and consequently, the dyestuff oxidation. Wolski et al. [14] reported a 51% degradation of Rhodamine B in 30 min using Nb_2O_5 with hydrogen peroxide, observing similar results, in terms of degradation efficiency, with the photocatalytic system at lower dye concentration. This appreciation is in good agreement with the findings documented by Ucker et al. [15].

No reports could be found in the literature on the effects of the operating conditions for textile wastewater treatment using a Nb_2O_5 monolithic catalyst in the presence of hydrogen peroxide. The use of structured catalysts is affordable considering that they can be reused in multiple cycles, overcoming the difficulty of separating the powder catalyst from the reaction medium, thus reducing processing costs.

In this paper, the oxidation of MB (as model dye compound) over an anodized aluminum-supported Nb_2O_5 catalyst in a monolithic stirrer reactor was studied. The effects of key parameters (catalyst loading, initial dye concentration, pH and initial hydrogen peroxide concentration) on the dye degradation and the stability of the monolith catalyst were evaluated.

Materials and methods

Catalyst synthesis

For the preparation of the anodized aluminum monoliths, an Al1050 commercial aluminum sheet was used as substrate (the composition of the aluminum sheets is given in Table S1 in the Supplementary Information). The aluminum sheets were washed with distilled water and acetone, then the anodizing process was carried out using a 1.6 M $H_2C_2O_4$ (≥ 99% purity; Sigma-Aldrich) aqueous solution as electrolyte and a power density of 2 A dm^{-2} at 40 °C, with 40 min of anodizing and 40 min of pore opening. After anodizing, the samples were washed with distilled water, dried and calcined at 450 °C for 120 min using chromatographic grade air (99.999% purity) with a flow rate of 20 mL min^{-1}. The monoliths were prepared by rolling around spindle alternate anodized a smooth and a corrugated sheet conforming sinusoidal channels. The final monolith was a cylinder of 14 mm diameter and 15 mm height (the geometric dimensions of the monolith are shown in the Table S2 in the Supplementary Information).

Nb_2O_5 (99% purity), provided by Brazilian Company of Minerals and Mineralization (CBMM), was dissolved in 1 M oxalic acid aqueous solution. The Nb_2O_5 monolith catalysts were synthesized by wet impregnation using a niobium aqueous solution (100 mM, pH 4) for 60 min. After impregnation, the samples were dried at room temperature for 48 h and finally calcined at 550 °C for 3 h in air flow (AGA chromatographic grade). Three impregnation, drying and calcination cycles were performed. The monolith catalysts are referred to as $Nb_2O_5/Al_2O_3/Al$.

Catalyst characterization

The $Nb_2O_5/Al_2O_3/Al$ catalysts were characterized using N_2 adsorption-desorption isotherms at − 196 °C for surface area measurements. The specific surface area of the catalysts was calculated according to BET method. The pore volume and pore size distribution of the samples were calculated from the N_2 adsorption isotherm with the BJH method, using a Quantachrome Instruments NOVA 1200e analyzer. Before the analysis, each sample was degassed in vacuum at 120 °C for 24 h.

The Nb_2O_5 loading in the monolith catalysts was determined by inductively coupled plasma-atomic emission spectroscopy (ICP-AES) with a Shimadzu 9000 spectrometer. Before the measurement, the samples were dissolved in aqua regia.

The catalyst morphology was characterized by scanning electron microscopy (SEM) on a LEO-EVO 40 XVP microscope. The samples were previously coated through a metallization process.

The adherence of the Nb_2O_5 layer deposited over the anodized aluminum surface was tested by the ultrasonic method. The monoliths were immersed in 50 mL of distilled water and subjected to an ultrasound bath at room temperature for 120 min in a Cole-Palmer 8892E-MT (47 kHz, 105 W) apparatus. Then the monoliths were dried. The weight of each sample was measured before and after the ultrasound test to determine the Nb_2O_5 layer adherence, which was calculated as the percentage ratio of the amount of coating material retained on the substrate.

X-Ray diffraction (XRD) was applied to identify the crystalline phases of the catalyst. XRD patterns were obtained using a Rigaku D-max III-C diffractometer, with a monochromatic Cu Kα (l = 0.154060 nm) operating at 35 kW and 30 mA.

Reaction test

The reaction tests were carried out at 20 ± 1 °C in a Pyrex batch reactor equipped with a monolith stirrer, in the dark. A schematic diagram of the monolithic stirrer

reactor used in the reaction tests and its characteristic parameters are given in Fig. S1 and Table S3 in the Supplementary Information. The duration of the reaction test was 150 min with an agitation rate of 500 rpm. In each test, 250 mL of MB (≥ 97% purity; Sigma-Aldrich) solution were used, and the catalytic monoliths were mounted on the axis of the stirrer. The pH of the reaction medium was regulated by adding 0.1 M HCl or 0.1 M NaOH solution (≥ 98% purity, Sigma-Aldrich reagents).

The reaction progress was monitored using a UV-VIS spectrophotometer (PG Instruments, T60). The wavelength selected for the measurement was 663 nm (maximum absorbance for MB), and the MB concentration was calculated using a calibration curve [9]. The MB degradation during the reaction test was determined using Eq. (1):

$$\text{MB degradation} = \frac{ABS_0 - ABS_F}{ABS_0}\ 100\% \tag{1}$$

where ABS_0 is the initial absorbance of MB solution, and ABS_F is the final absorbance (after the reaction test). The efficiency of the oxidation process was also evaluated in terms of COD reduction as follows:

$$\text{COD red} = \frac{\text{COD}_0 - \text{COD}_F}{\text{COD}_0}\ 100\% \tag{2}$$

where COD_0 is the initial COD (untreated sample) and COD_F is the COD of the sample treated by the advanced oxidation process. COD analysis was carried out using commercial HACH vials (Method 8000). The samples were prepared using sulfuric acid and potassium dichromate as oxidizing agent at 150 °C for 120 min.

Experimental design

The effects of the operating conditions on the reaction tests were investigated using a central composite design (CCD) at three levels together with response surface methodology. The CCD consisted of a 2^4 factorial design with 2 center point replicates, resulting in 18 catalytic tests. This method is suitable for fitting a quadratic surface by analyzing the interactions between the parameters with a minimum number of experiments. The central points were used to determine the experimental error and the reproducibility of the results. The independent variables were pH, initial concentration of MB ($C_{MB,\ 0}$) and hydrogen peroxide ($C_{H_2O_{2,0}}$), and catalyst loading (ω), which were coded to the (− 1,1) interval, where the low and high levels are coded as − 1 and + 1, respectively. The indepeFndent variables with their respective ranges were selected based on the literature as listed in Table 1. The order of the experiments was randomized in order to minimize the effects of the uncontrolled factors.

Table 1 Independent variables and their coded levels for the central composite design

Variables	Code	Units	Coded levels		
			-1	0	1
pH	x_1	–	4	6	8
$C_{MB,\ 0}$	x_2	(mg L^{-1})	15	30	45
$C_{H_2O_{2,0}}$	x_3	(mM)	40	60	80
ω	x_4	($kg_{Nb_2O_5}$ m^{-3})	2.62	5.24	7.86

The studied responses were MB degradation, Eq. (1) and COD reduction, Eq. (2). The responses were fitted by multiple regression, and the generated models were used to evaluate the effects of the selected experimental factors according to Eq. (3):

$$Y = b_0 + \sum_{i=1}^{4} b_i x_i + \left(\sum_{i=1}^{4} b_{ii} x_i\right)^2 + \sum_{i=1}^{3}\sum_{j=i+1}^{4} b_{ij} x_i x_j \tag{3}$$

where Y is the predicted response, b_0 is the constant coefficient, b_i is the linear coefficient, b_{ij} is the interaction coefficient, b_{ii} is the quadratic coefficient, and $x_i x_j$ are the values of the independent variables. Analysis of variance was used to evaluate the adequacy of the predicted model using Statgraphics Centurion XV.2 software. The quadratic model was adjusted by stepwise selection according to the Fisher-Snedecor test (F-test) in order to remove statistically non-significant variables. The goodness of fit was assessed using the coefficient of determination (R^2). Non-significant coefficients were removed from the models (p-value > 0.05).

Results and discussion

Catalyst characterization

Figure 1 shows the nitrogen adsorption–desorption isotherm for $Nb_2O_5/Al_2O_3/Al$ monolith catalyst. The isotherm is of type IV according to the IUPAC classification, indicating the presence of mesopores. It presents a hysteresis loop, which may be attributed to capillary condensation in the pores.

The BET surface area of the monolith catalysts was of 43 $m^2\ g^{-1}$, with a pore radius of 179 Å and a pore volume of 0.011 $cm^3\ g^{-1}$ (values referring to the Nb_2O_5 loading in the monolith). These properties were in good agreement with the results reported by Ohuchi et al. [16] for a Nb_2O_5 catalyst synthetized through niobic acid calcination.

Figure 2 shows the XRD patterns of anodized aluminium monoliths and $Nb_2O_5/Al_2O_3/Al$ catalyst. The

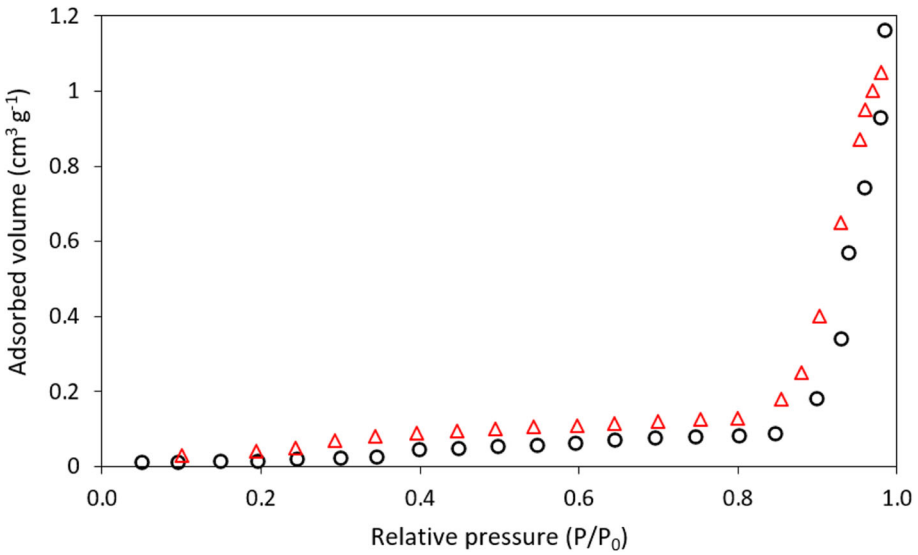

Fig. 1 N_2 adsorption-desorption isotherm for $Nb_2O_5/Al_2O_3/Al$ monolith catalyst. Ref.: Adsorption, Desorption

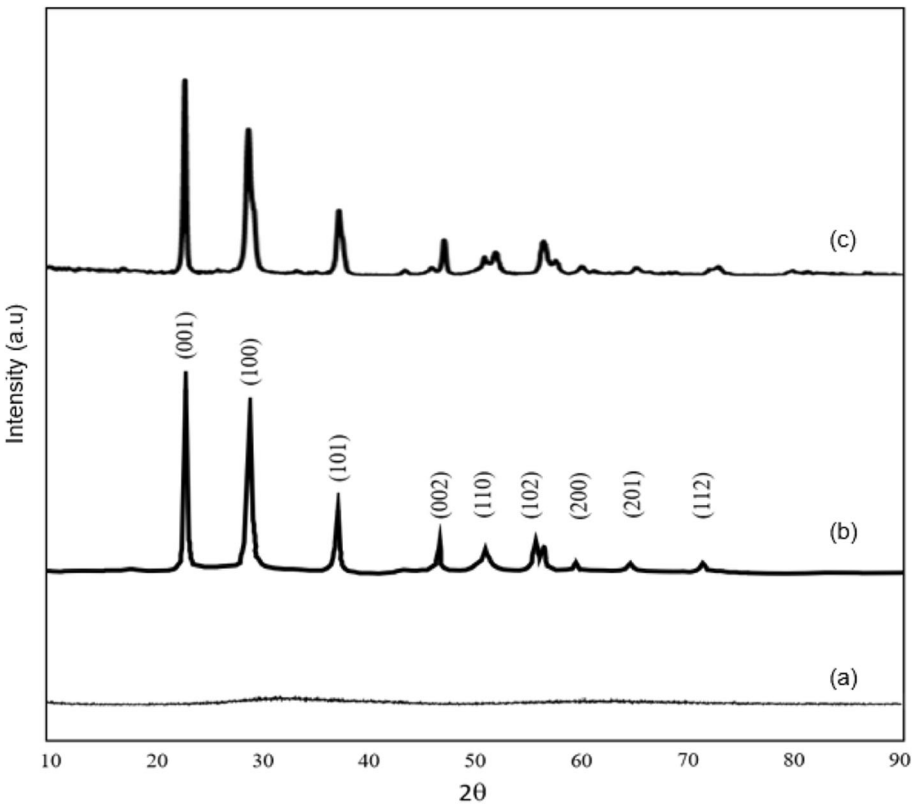

Fig. 2 XRD patterns: (**a**) anodic alumina generated during the anodizing process, (**b**) reference TT-Nb_2O_5 (JCPDS 28–0317), (**c**) $Nb_2O_5/Al_2O_3/Al$ monolith

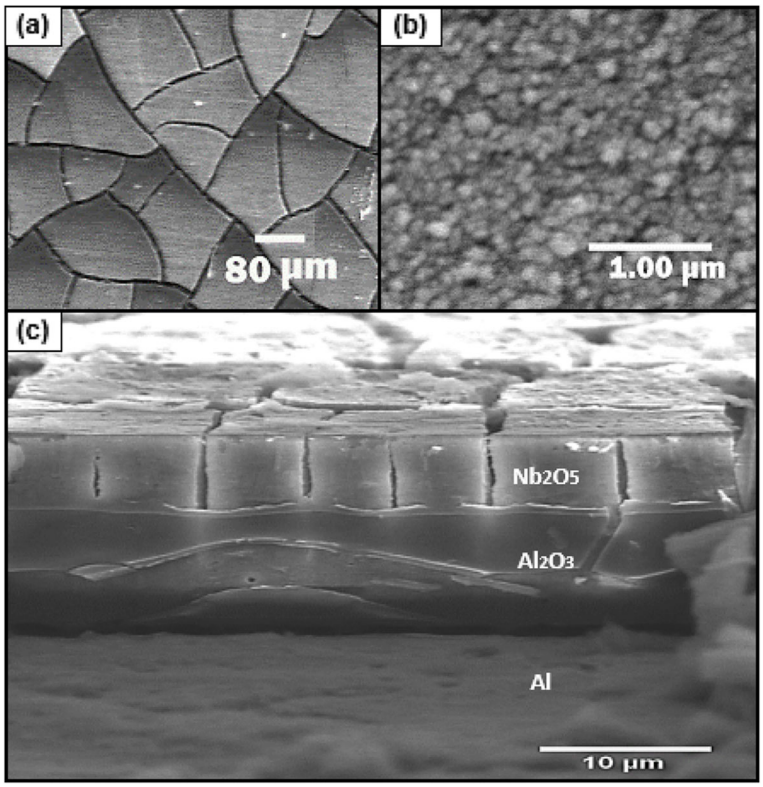

Fig. 3 SEM micrographs of $Nb_2O_5/Al_2O_3/Al$ monolith. Ref.: (**a**), (**b**): Top view; (**c**): Vertical cross-section

crystallographic planes were identified according to JCPDS database. The alumina generated during the anodization process exhibited an amorphous structure, which is in good agreement with the results previously reported by Zhao et al. under similar anodization conditions [17]. On the other hand, the $Nb_2O_5/Al_2O_3/Al$ catalyst showed well defined peaks, indicating the presence of a crystalline TT-Nb_2O_5 phase (JCPDS file shown in Fig. 2B). Nb_2O_5 exhibited different crystalline phases as the temperature increased, showing polyhedral distortion. The TT phase presented a slight distortion of the polyhedra with respect to the hexagonal structure, adopting a pseudo hexagonal structure when the temperature was increased up to 500 °C [18].

The Nb_2O_5 loading of the monolith catalyst was determined by ICP-AES, being of 327 $mg_{Nb_2O_5}$ $monolith^{-1}$. The monoliths were subjected to ultrasound testing to determine the adherence the of Nb_2O_5 layer deposited over anodized aluminum substrate. The coating adherence was found to be excellent (99.8 ± 0.1%). The results are in agreement with those presented by Koyama et al. [19], who deposited a highly stable Nb_2O_5 layer over anodized aluminum by a sol-gel coating method. Feng et al. [20] also obtained Al_2O_3-Nb_2O_5 composite oxide films with high adherence following a similar preparation procedure to that used in this work. Figure 3 shows SEM micrographs of the surface of $Nb_2O_5/Al_2O_3/Al$ catalyst and a cross-section of the Nb_2O_5 deposited layer.

The surface of the Nb_2O_5 layer was homogeneous, with a thickness of 7 µm, while the thickness of the Al_2O_3 layer was of 17 µm. The coating exhibited a rough surface, occasionally divided by cracks that went from the surface down to the alumina matrix. This morphology has also been observed by other authors and it may be attributed to shrinkage during the preparation drying stage [21].

The solubility of Nb_2O_5 in aqueous solutions depends on its crystalline structure, temperature, pH and ionic strength [22]. The Nb_2O_5 obtained from the alkalization-precipitation of a niobium oxalate solution exhibits an amorphous structure, with a relatively high solubility in water [23]. However, when Nb_2O_5 is calcined at temperatures above 500 °C, a TT-Nb_2O_5 crystalline phase is generated, decreasing the dissolution rate.

Figure 4 shows the dissolution of Nb_2O_5 after 150 min of reaction at different pH. The samples of the reaction medium were collected and analyzed by ICP-AES to determine the niobium concentration. Figure 4 compares the results for Nb_2O_5 dissolution (from the Nb_2O_5/

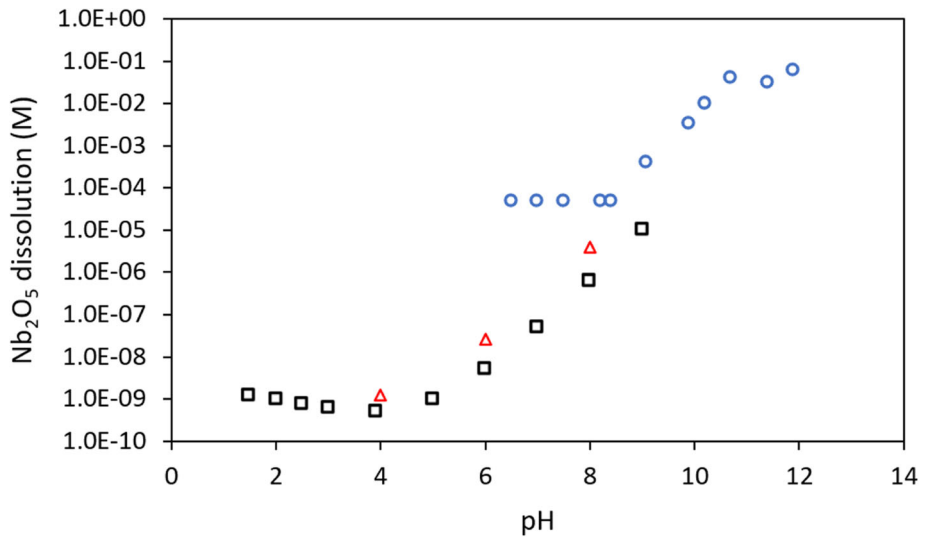

Fig. 4 Nb_2O_5 dissolution in an aqueous medium versus pH at room temperature. Ref.: Amorphous Nb_2O_5 [24], H-Nb_2O_5 [25], $Nb_2O_5/Al_2O_3/Al$ (present work)

Al_2O_3/Al catalyst) found in this work with those reported by other authors [22, 26] as a function of pH (at room temperature).

As shown in Fig. 4, the dissolution was significantly lower for TT-Nb_2O_5 than for the amorphous material. In all cases, an increase in pH yielded an increase in Nb_2O_5 dissolution for pH 4–12. Based on these results, it was assumed that the reaction only occurred over Nb_2O_5 surface and the niobia dissolution was negligible. This is in agreement with the results reported by Peiffert et al. for H-Nb_2O_5 [22].

Timofeev et al. [27] studied the dissolution of Nb_2O_5 at high temperatures in acid media and reported a solubility of $10^{-7.8}$ M at 150 °C and pH 2. Deblonde et al. [26] reported a niobium dissolution of $10^{-3.5}$ M for 56-d aged niobium hydroxide at 25 °C and pH 9. Peiffert et al. [22] examined the solubility of anhydrous Nb_2O_5 at different temperatures and ionic strengths. The highest value reported by the authors for an ionic strength value of 0.1 M ($NaClO_4$) at 25 °C was of 6.0 10^{-10} M. Korzhinskaya et al. [23] found a solubility limit value of 8.3 10^{-6} M for Nb_2O_5 calcined at 550 °C, at pH 5 and 0.01 M (Na_2CO_3). It was proposed that niobium oxide dissolution is independent of the ionic strength, between 0.1 and 1 M, and pH 3–8, at room temperature [28].

Catalytic tests

Mass transport phenomena

The Carberry (Ca) criterion was used to evaluate the external mass transfer limitation in the liquid-solid film according to Eq. (4). The external mass transfer resistance is negligible when Ca < 0.05.

$$\mathrm{Ca} = \frac{\mathrm{r}_{\mathrm{liq}}^{\mathrm{obs}}}{\mathrm{k}_{\mathrm{LSi}}\mathrm{a}_{\mathrm{LS}}\,\mathrm{C}_{\mathrm{i}}} \tag{4}$$

where C_i is the concentration of MB or H_2O_2 (mol m^{-3}) and r_{liq}^{obs} is the observed reaction rate (mol m^{-3} s^{-1}). The liquid-solid mass transfer area (a_{LS}) was calculated from the dimensions of the Al sheets that made up the monoliths as 3834 m^2 m^{-3}. The liquid-solid mass transfer coefficient was determined according to the correlation proposed by Butler et al. [29] as k_{LSMB} = 3.85 10^{-5} m s^{-1} and $k_{LSH_2O_2}$ = 2.34 10^{-4} m s^{-1}. The Carberry criterion indicated that the resistance to external mass transfer was negligible for MB and hydrogen peroxide (all the results are shown in Table S4 in Supplementary Information).

The Weisz-Prater criterion, Eq. (5) was used to estimate the intraparticle diffusion limitation for both methylene blue and hydrogen peroxide.

$$\Phi_{\mathrm{i}} = \frac{\mathrm{r}_{\mathrm{cat}}^{\mathrm{obs}}\rho_{\mathrm{c}}\,\mathrm{L}^2}{\mathrm{D}_{\mathrm{eff,i}}\mathrm{C}_{\mathrm{i}}} \tag{5}$$

where D_{eff} is the effective diffusion coefficient (m^2 s^{-1}), L is the thickness of the Nb_2O_5 layer (m), and ρ_c is the apparent density of the catalyst (kg m^{-3}). The effective diffusion coefficient was calculated as follows:

$$\mathrm{D}_{\mathrm{eff,i}} = \frac{\mathrm{D}_{\mathrm{i}}\,\varepsilon}{\tau} \tag{6}$$

The Weisz-Prater criterion indicates that the intraparticle mass transfer limitation for the unknown kinetics is negligible when Φ_i < 0.1. The Nb_2O_5 porosity was ε = 0.22 and the tortuosity was τ = 3 [5]. Intraparticle

diffusion coefficients were determined using the correlation proposed by Milozic et al. [24] as D_{MB} = 4.75 10^{-10} m^2 s^{-1} and as $D_{H_2O_2}$ = 7.1 10^{-9} m^2 s^{-1}. The catalyst density was assumed to be 1220 kg m^{-3}. The thickness of the Nb_2O_5 layer was 7 μm.

Under the reaction conditions analyzed in this work, the numerical value of the Weisz-Prater criterion was between 0.8 and 4.2 for MB and between 0.5 and 6.4 10^{-4} for H_2O_2, indicating that the concentration gradients within the catalyst pores for MB cannot be neglected (all the results are shown in Table S4 in the Supplementary Information). This may be attributed to the low effective diffusivity coefficient of methylene blue for the reaction system. Meanwhile, the intraparticle diffusion limitations for H_2O_2 were negligible.

Effects of the operating conditions on the studied reaction

In this study a central composite design was developed to determine the optimal conditions for MB degradation and COD reduction. The independent variables were: pH, initial concentration of MB ($C_{MB,\ 0}$) and hydrogen peroxide ($C_{H_2O_{2,0}}$), and catalyst loading (ω). Table 2 shows the complete design matrix together with the values of both responses obtained from the experimental tests.

In order to clarify the contribution of the Fenton-like reaction in MB degradation, the dye was contacted with the H_2O_2, without catalyst, and no degradation was observed. When the H_2O_2 was contacted with the catalyst, no O_2 formation was observed. Both experiments suggest the possible formation of hydroxyl radicals, which would be responsible for the oxidation of MB over Nb_2O_5 in the presence of H_2O_2. The contribution of the Fenton-like reaction was also proposed by Oliveira et al. [13], whose results strongly suggest that the reaction with Nb_2O_5 catalyst is initialized by the activation of H_2O_2 to produce •OH radicals.

Under the studied operating conditions and at 150 min of reaction, the minimum MB degradation obtained was 75%, with a COD reduction of 11% (Run 14) or 23% (Run 12). On the other hand, the maximum MB degradation was of 98% with a COD reduction of 79% (Run 1 and 5). Similar results were obtained for both reaction tests at the central point (Run 2 and 11), indicating that the assays were reproducible.

The results of each response were adjusted to a second-order model, using the F-test to remove statistically insignificant variables. Table 3 shows the equations obtained by multiple regression, the percentages of variation of the parameters explained by R^2, the *p*-values and the F-values. The coded values for the variables are those presented in Table 1.

The coefficient of determination (R^2) obtained for COD reduction and MB degradation was 0.795 and 0.986, respectively. Both second-order models showed p-

Table 2 Experimental variables and responses for MB degradation using $Nb_2O_5/Al_2O_3/Al$ catalyst

Run	x_1: pH	x_2 : $C_{MB,\ 0}$ (mg L^{-1})	x_3 : $C_{H_2O_{2,0}}$ (mM)	x_4 : ω ($kg_{Nb_2O_5}$ m^{-3})	Y_1:MB degradation (%)	Y_2:COD reduction (%)
1	4	15	40	7.86	98	79
2*	6	30	60	5.24	88	55
3	4	45	40	2.62	93	43
4	4	45	80	7.86	96	91
5	4	45	40	7.86	98	78
6	4	15	80	2.62	91	57
7	4	15	80	7.86	97	73
8	8	15	40	7.86	94	88
9	4	45	80	2.62	91	22
10	4	15	40	2.62	90	32
11*	6	30	60	5.24	89	53
12	8	45	80	2.62	75	22
13	8	15	40	2.62	78	15
14	8	15	80	2.62	75	10
15	8	15	80	7,86	91	75
16	8	45	40	7.86	94	55
17	8	45	40	2.62	80	26
18	8	45	80	7.86	90	42

*Central point

Table 3 Mathematical models obtained using Statgraphics Centurion XV.2 software for the studied responses. All data had a confidence level of over 95.0%

Response	Mathematical models*	Eq.	R^2	*p*-Value	F-Value
MB degradation	$Y_1(\%) = 107.02 - 4.08\ x_1 - 0.0106\ x_1\ x_3 + 0.4412\ x_1\ x_4 - 0.6202\ x_4$	7	0.986	0.0001	322
COD reduction	$Y_2\ (\%) = 33.77 - 4.43\ x_1 + 8.42\ x_4$	8	0.795	0.0001	29

* x_1: pH, x_2: initial methylene blue concentration, x_3: initial hydrogen peroxide concentration, x_4: catalyst loading

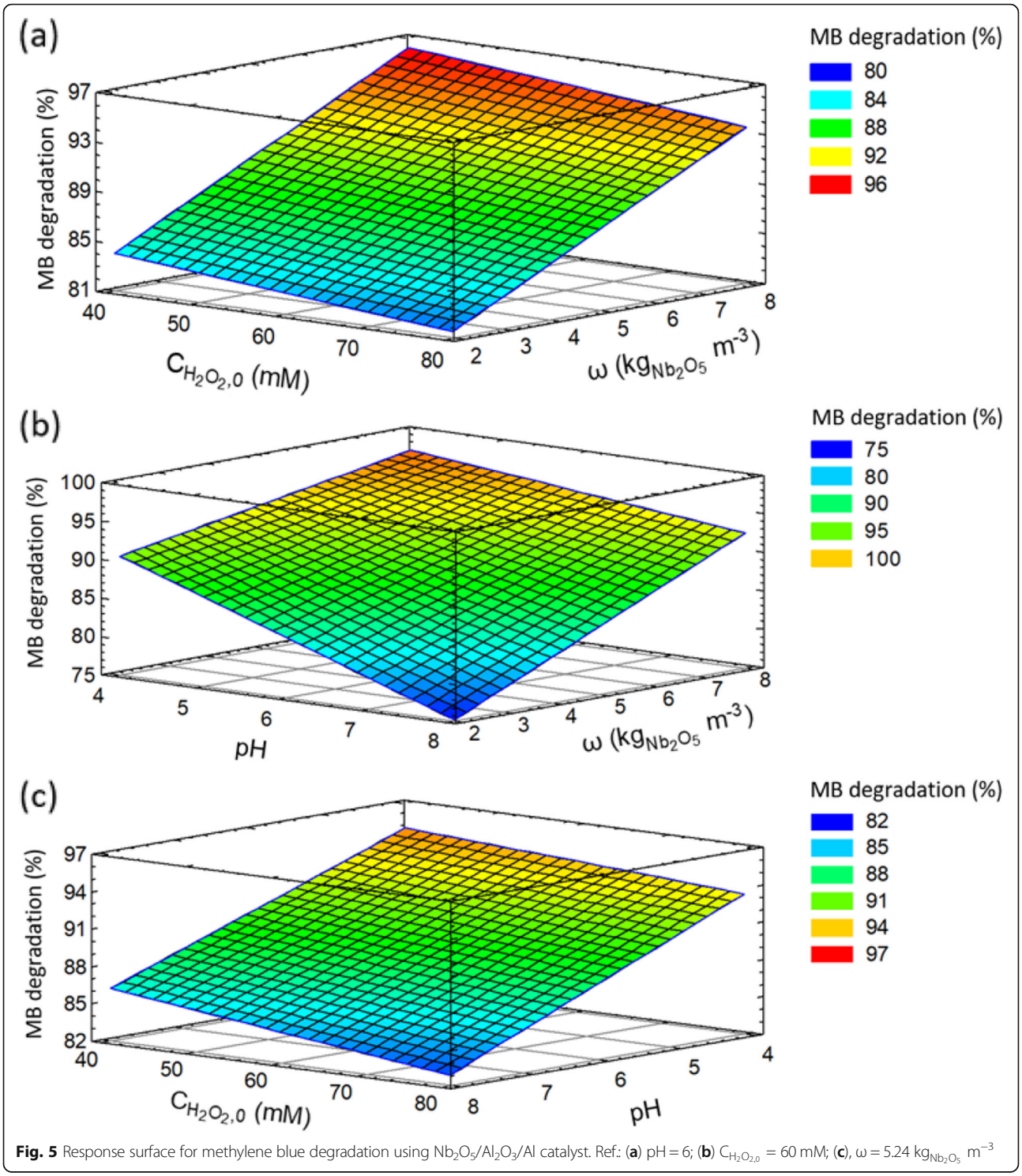

Fig. 5 Response surface for methylene blue degradation using $Nb_2O_5/Al_2O_3/Al$ catalyst. Ref.: (**a**) pH = 6; (**b**) $C_{H_2O_2,0}$ = 60 mM; (**c**), ω = 5.24 $kg_{Nb_2O_5}$ m^{-3}

values lower than 0.05, ensuring a satisfactory fit of the experimental data with a confidence level greater than 95%. Three-dimensional response surface curves were plotted to understand the interactions between the parameters. Figure 5 shows the response surfaces for MB degradation as a function of two independent variables, and the third and fourth variables were fixed at level "0", as specified in Table 4. Figure 6 shows the response surface for COD reduction.

The effects of the operating conditions for MB degradation and COD reduction are discussed below.

a. pH

The influence of pH on MB degradation and COD reduction was studied in the 4–8 pH range. Both responses were favored by lower pH and higher catalyst loadings. As shown in Fig. 5b, an increase in catalyst loading led to a decrease in the pH effect on MB degradation. This behavior has been reported by other authors and it may be attributed to the predominant effect of catalyst loading in the reaction system [10, 30].

The pH presents various effects on the reaction system, and it can affect the catalyst surface and/or the reactants, and thus its analysis can sometimes be complex. Changes in pH can alter the adsorption process of the organic molecules on the catalyst surface, which is the first step of the reaction. The isoelectric point of the Nb_2O_5 coating was $pH_{pzc} = 6.8$. At $pH > pH_{pzc}$, the total surface of the Nb_2O_5 monolith catalyst was negatively charged, whereas at $pH < pH_{pzc}$ the surface had a net positive charge, as shown in the following equations:

$$pH > 6.8 : Nb{-}OH + OH^{-} \leftrightarrow Nb{-}O^{-}H_2O \quad (7)$$

$$pH < 6.8 : Nb{-}OH + H^{+} \leftrightarrow Nb{-}OH_2^{+} \quad (8)$$

MB is a cationic dye and its adsorption over the niobia surface by electrostatic interaction is favored at pH > 6.8, as indicated in Fig. 7a. However, there are other possible interactions at low pH between the reactants and the catalyst: a) Lewis acid-base interaction between the axial nitrogen atom of the MB molecule and Nb^{+5} sites on the surface (Fig. 7b), b) hydrogen bonding between the nitrogen atom of the central aromatic ring and niobia surface (Fig. 7c), and c) π interaction between the aromatic rings and the niobia surface (Fig. 7d) [25, 31].

Oliveira et al. [10, 13] proposed that hydrogen peroxide molecules are adsorbed over niobia forming peroxo-niobium groups, which are potential oxygen donors. The hydrogen peroxide adsorption on the catalyst surface is also influenced by pH. Wang et al. [32] studied the aerobic oxidation of alcohols by UV radiation using TiO_2 catalyst, observing the formation of peroxo-niobium groups. When a Brønsted acid is present, H^+ are adsorbed on the catalyst surface, weakening the O-O bond of the peroxo-niobium groups, and thus promoting their heterolytic hydrolysis. In this sense, it can be inferred that under the reaction conditions evaluated in the present work, a decrease in pH led to the regeneration of the active sites on the niobia surface, favoring MB adsorption and its subsequent degradation.

The COD value no depends on the concentration of products and reagents. As shown in Fig. 6, an increase in pH had a negative effect on COD reduction. As stated above, the heterolytic hydrolysis of peroxo-niobium groups is promoted at lower pH, favoring H_2O_2 decomposition, and consequently increasing COD reduction [10].

b. Catalyst concentration

An improvement in MB degradation and COD reduction was observed when the catalyst loading was increased from 2.62 to 7.68 $kg_{Nb_2O_5}\ m^{-3}$. This behavior may be attributed to the increase in total vacant adsorption sites on the Nb_2O_5 surface, thus favoring the adsorption of MB and H_2O_2. It was also observed that an increase in the catalyst loading yielded a greater hydroxyl (•OH) radical generation when hydrogen peroxide was used as oxidant reagent, hence improving dyestuff degradation [32].

c. Initial concentration of reagents

In the present study, the initial dye concentration was between 15 and 45 $mg\,L^{-1}$. According to the results obtained, MB degradation was no sensitive to initial dye concentration. As shown in Fig. 5A and C, MB degradation was favored by decreasing the initial hydrogen peroxide concentration. This can be explained considering that hydrogen peroxide reagent was in excess in the reaction medium, hence a decrease in H_2O_2 concentration favored dye adsorption, and subsequently MB degradation.

On the other hand, no statistically significant relationships between COD reduction and initial concentration

Table 4 COD values for standard samples

Sample	$C_{MB,\,0}$ ($mg\,L^{-1}$)	$C_{H_2O_{2,0}}$ (mM)	COD ($mg\,L^{-1}$)
1	15	40	504
2	15	80	936
3	45	40	570
4	45	80	1024
5	0	40	566
6	0	80	920
7	15	0	8
8	30	0	36
9	45	0	47

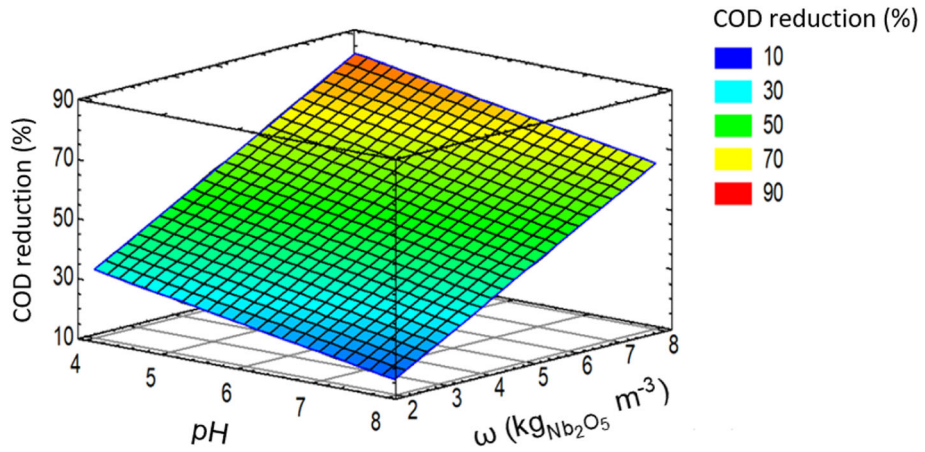

Fig. 6 Response surface for COD reduction using $Nb_2O_5/Al_2O_3/Al$ catalyst

of the reagents were determined. Optimal hydrogen peroxide concentration for textile wastewater treatment depends on effluent composition and operating conditions [33].

The COD of standard samples was determined to quantify the influence of MB and H_2O_2 concentrations during COD measurement. The results are presented in Table 4, and they indicate that hydrogen peroxide had a predominant contribution to the COD value. Kang et al. [34] evaluated the interference of hydrogen peroxide on standard COD tests. They proposed the following equation, which can be applied to hydrogen peroxide concentrations in the 0–2000 mg L^{-1} range, to correct the effect of the hydrogen peroxide concentration on COD:

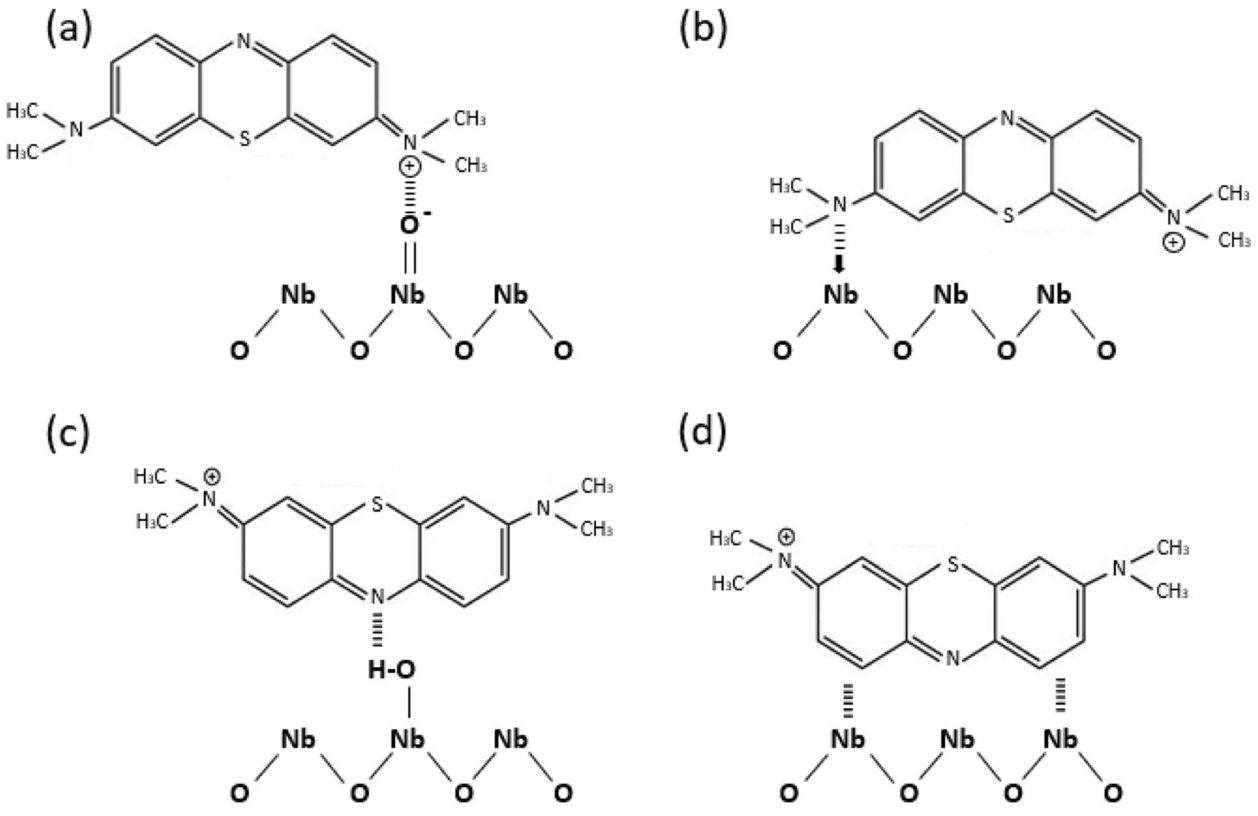

Fig. 7 MB molecule adsorption mechanisms over niobia surface. Ref.: (**a**) electrostatic interaction, (**b**) Lewis acid-base interaction, (**c**) hydrogen bond interaction, (**d**) interaction by delocalized π electrons

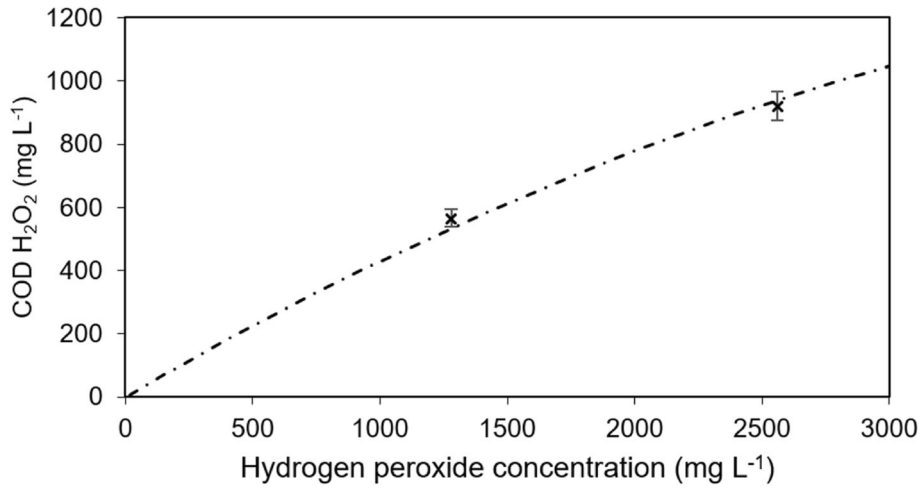

Fig. 8 Experimental (symbols) and modelled data (according to Eq. (9), dotted line) for COD test as a function of hydrogen peroxide concentration

$$\text{COD } H_2O_2 = 0.4706\ C_{H_2O_2} - 4.06\ 10^{-5} C_{H_2O_2}{}^2 \qquad (9)$$

where $C_{H_2O_2}$ is the hydrogen peroxide concentration expressed in mg L^{-1}. Figure 8 shows the COD values calculated according to Eq. (9) and those of Table 4, as a function of hydrogen peroxide concentration.

The COD values obtained in the present work for hydrogen peroxide (samples 5 and 6 of Table 4) were in good agreement with those calculated by Eq. (9), indicating that the COD value is mainly determined by H_2O_2 concentration.

Based on these results, the optimal operating conditions selected for MB degradation and COD reduction using $N_2O_5/Al_2O_3/Al$ monolith catalyst were: pH 4, $C_{H_2O_{2,0}}$ = 40 mM, $C_{MB,\ 0}$ = 45 mg L^{-1}, and $\omega = 7.86$ $kg_{Nb_2O_5}$ m^{-3}.

Yahiaoui et al. [35] observed, at a similar MB degradation found in this work (under optimal operating conditions), a substantial increase in the BOD/COD ratio of the effluent after the oxidation process, indicating an increase in its biodegradability. Similar observations were reported by Sapawe et al. [36].

Oliveira et al. [13] proposed a tentative reaction mechanism for the MB degradation over niobia catalyst. The intermediate species were identified by on-line electrospray ionization mass spectrometry, and these results were interpreted with the assistance of the calculation of the Gibbs free energy of the intermediate species. The authors indicated that the reaction is initiated with the activation of H_2O_2 by niobia via Haber Weiss mechanism, followed by the consecutive hydroxylation of the aromatic ring at position C2, C4 and C5. This is a critical step, as it would simultaneously lead to the formation of hydroquinone or hydroquinone-like intermediates generated by the •OH attack. This would be an unstable key-intermediate that points out the quick and high probability of rupture of both chemical bonds C1–C2 and C5–C6, followed by its oxidation generating a stable species, with m/z = 160.

Kinetic model

Under optimal conditions, the decolorization of MB follows pseudo first-order kinetics according to Eq. (10) [15]:

$$C_{MB} = C_{MB,0} e^{\left(-k' t\right)} \quad \text{or} \quad \ln\left(\frac{C_{MB}}{C_{MB,0}}\right) = -k' t \qquad (10)$$

where $C_{MB,\ 0}$ is the initial concentration of MB (mg L^{-1}), C_{MB} is the dye concentration at various time intervals, t is the reaction time (min), and k' is the pseudo first-order rate constant (min^{-1}). By plotting $-\ln(C_{MB} / C_{MB,\ 0})$ vs t, it is possible to calculate the apparent rate constant for MB degradation. Figure 9 presents the experimental and modelled data versus reaction time for MB degradation under optimal conditions.

Figure 9 shows that the experimental data were satisfactorily adjusted with Eq. (10) (R^2 = 0.983), demonstrating that the decolorization reaction followed a pseudo first-order kinetics, with an apparent rate constant of ~ 0.03 min^{-1}. This value is in good agreement with that reported by Khairnar et al. under similar operating conditions [37].

Catalyst stability test

One of the main advantages of monolith catalysts is the possibility to separate them easily from the reaction medium and use them repeatedly. In this context, the stability of the catalyst activity through consecutive uses is an important factor. To the best of our knowledge, no

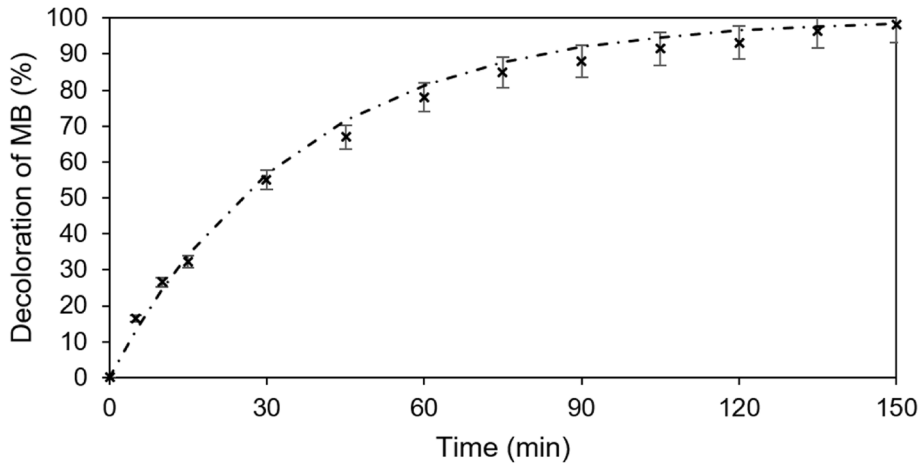

Fig. 9 Experimental (symbols) and modelled data (dotted line) for MB degradation using $Nb_2O_5/Al_2O_3/Al$ catalyst under optimal operating conditions

studies have been reported in the literature about the stability of Nb_2O_5 on monolith supported catalysts.

Multiple consecutive reaction tests under optimal operating conditions with $Nb_2O_5/Al_2O_3/Al$ catalyst were carried out to analyze the effects of reuse on catalyst activity. The tests were performed using MB solution (in distilled water) and a model textile wastewater, whose composition was: 45 mg L^{-1} MB, 5 mg L^{-1} NH_4^+, 778 mg L^{-1} Na^+, 700 mg L^{-1} Cl^-, 5 mg L^{-1} NO_3^- and 150 mg L^{-1} SO_4^{-2} [38]. No treatment was performed in the structured catalysts between the tests.

Figure 10 shows the dye degradation for ten consecutive tests for MB solution and model textile wastewater treatment. The monolith catalyst reached similar percentages of MB degradation for both cases, and the catalyst activity remained virtually constant after ten consecutive uses. XRD analysis before and after the 10 catalyst stability test were performed in order to explore possible changes in the crystalline structure of the niobia (data shown in Supplementary Information, Fig. S2). The results indicated that the Nb_2O_5 layer over the anodized aluminum monolith remained unaltered.

Conclusions

The Nb_2O_5 coating was successfully deposited over an anodized aluminum substrate, showing excellent adherence. The morphology of the surface of the Nb_2O_5 layer was homogeneous and porous, with a thickness of 7 μm. The dissolution of Nb_2O_5 in aqueous solution was negligible as a function of pH at room temperature. The

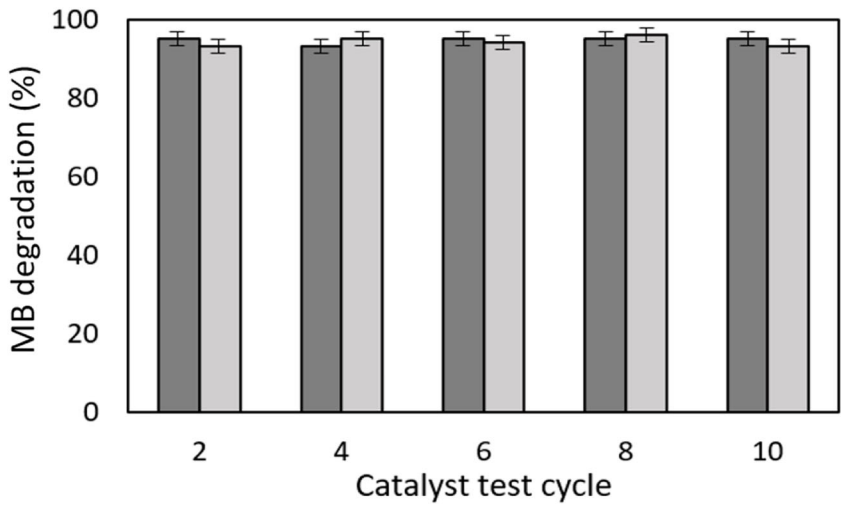

Fig. 10 MB degradation reached after 150 min of reaction under optimal conditions using $Nb_2O_5/Al_2O_3/Al$ catalyst. Ref: MB solution (distilled water), Model textile wastewater

lowest value for Nb_2O_5 dissolution was 1.25 10^{-9} M Nb (pH 4), and the highest value was 3.98 10^{-6} M Nb (pH 8). A central composite design was developed to analyze the effect of the operating conditions on dye degradation and COD reduction. The experimental results were satisfactorily adjusted by multiple regression model. The optimal reaction conditions were: pH = 4, $C_{H_2O_{2,0}}$ = 40 mM, $C_{MB,\,0}$ = 45 mg L^{-1}, and ω = 7.86 $kg_{Nb_2O_5}$ m^{-3}. The $Nb_2O_5/Al_2O_3/Al$ catalyst maintained its high catalyst activity after ten consecutive uses.

Supplementary Information

The online version contains supplementary material available at https://doi.org/10.1186/s42834-021-00109-4.

Additional file 1.

Acknowledgements

The authors are thankful to CBMM-Brazil for the donation of the Nb_2O_5.

Authors' contributions

The corresponding author GMT has conceptualized and designed the study, also supervised in manuscript writing and data interpretation. The first author FDT have performed lab work as well as the manuscript writing. Both authors have read and approved the final manuscript.

Funding

The work was supported by the Agencia Nacional de Promoción Científica y Tecnológica (National Agency of Scientific and Technological Promotion, Argentina), the Universidad Nacional del Sur, and the Consejo Nacional de Investigaciones Científicas y Técnicas (National Council for Scientific and Technological Research, CONICET).

Availability of data and materials

Not Applicable.

Declarations

Competing interests

The authors declare they have no competing interests.

Received: 27 March 2021 Accepted: 27 September 2021
Published online: 19 October 2021

References

1. Gumus D, Akbal F. Photocatalytic degradation of textile dye and wastewater. Water Air Soil Poll. 2011;216:117–24.
2. Holkar CR, Jadhav AJ, Pinjari DV, Mahamuni NM, Pandit AB. A critical review on textile wastewater treatments: possible approaches. J Environ Manage. 2016;182:351–66.
3. Pazdzior K, Bilinska L, Ledakowicz S. A review of the existing and emerging technologies in the combination of AOPs and biological processes in industrial textile wastewater treatment. Chem Eng J. 2019;376:120597.
4. Khan SH, Yadav VK. Advanced oxidation processes for wastewater remediation: an overview. In: Shah MP, editor. Removal of emerging contaminants through microbial processes. Singapore: Springer; 2021. p. 71–93.
5. Nakajima K, Fukui T, Kato H, Kitano M, Kondo JN, Hayashi S, et al. Structure and acid catalysis of mesoporous $Nb_2O_5{\cdot}nH_2O$. Chem Mater. 2010;22:3332–9.
6. de Carvalho GSG, de Siqueira MM, do Nascimento MP, de Oliveira MAL, Amarante GW. Nb_2O_5 supported in mixed oxides catalyzed mineralization process of methylene blue. Heliyon. 2020;6:04128.
7. Souza RP, Freitas TKFS, Domingues FS, Pezoti O, Ambrosio E, Ferrari-Lima AM, et al. Photocatalytic activity of TiO_2, ZnO and Nb_2O_5 applied to degradation of textile wastewater. J Photoch Photobio A. 2016;329:9–17.
8. Kumari N, Gaurav K, Samdarshi SK, Bhattacharyya AS, Paul S, Rajbongshi B, et al. Dependence of photoactivity of niobium pentoxide (Nb_2O_5) on crystalline phase and electrokinetic potential of the hydrocolloid. Sol Energ Mat Sol C. 2020;208:110408.
9. Prado AGS, Bolzon LB, Pedroso CP, Moura AO, Costa LL. Nb_2O_5 as efficient and recyclable photocatalyst for indigo carmine degradation. Appl Catal B-Environ. 2008;82:219–24.
10. Oliveira LCA, Goncalves M, Guerreiro MC, Ramalho TC, Fabris JD, Pereira MC, et al. A new catalyst material based on niobia/iron oxide composite on the oxidation of organic contaminants in water via heterogeneous Fenton mechanisms. Appl Catal A-Gen. 2007;316:117–24.
11. Ziolek M, Sobczak I, Decyk P, Wolski L. The ability of Nb_2O_5 and Ta_2O_5 to generate active oxygen in contact with hydrogen peroxide. Catal Commun. 2013;37:85–91.
12. Cardoso FP, Nogueira AE, Patricio PSO, Oliveira LCA. Effect of tungsten doping on catalytic properties of niobium oxide. J Brazil Chem Soc. 2012;23:702–9.
13. Oliveira LCA, Ramalho TC, Goncalves M, Cereda F, Carvalho KT, Nazzarro MS, et al. Pure niobia as catalyst for the oxidation of organic contaminants: mechanism study via ESI-MS and theoretical calculations. Chem Phys Lett. 2007;446:133–7.
14. Wolski L, Walkowiak A, Ziolek M. Photo-assisted activation of H_2O_2 over Nb_2O_5 – The role of active oxygen species on niobia surface in photocatalytic discoloration of Rhodamine B. Mater Res Bull. 2019;118:110530.
15. Ucker CL, Goetzke V, Almeida SR, Moreira EC, Ferrer MM, Jardim PLG, et al. Photocatalytic degradation of rhodamine B using Nb_2O_5 synthesized with different niobium precursors: factorial design of experiments. Ceram Int. 2021;47:20570–8.
16. Ohuchi T, Miyatake T, Hitomi Y, Tanaka T. Liquid phase photooxidation of alcohol over niobium oxide without solvents. Catal Today. 2007;120:233–9.
17. Zhao NQ, Jiang XX, Shi CS, Li JJ, Zhao ZG, Du XW. Effects of anodizing conditions on anodic alumina structure. J Mater Sci. 2007;42:3878–82.
18. Ucker CL, Riemke FC, Neto NFD, Santiago ADG, Siebeneichler TJ, Carreno NL, et al. Influence of Nb_2O_5 crystal structure on photocatalytic efficiency. Chem Phys Lett. 2021;764:138271.
19. Koyama S, Kikuchi T, Sakairi M, Takahashi H, Nagata S. Nb_2O_5 deposition on aluminum from $NbCl_5$-used sol and anodizing of Nb_2O_5-coated Al. Electrochemistry. 2007;75:573–5.
20. Feng ZS, Chen JJ, Zhang R, Zhao N. Formation of Al_2O_3-Nb_2O_5 composite oxide films on low-voltage etched aluminum foil by complexation-precipitation and anodizing. Ceram Int. 2012;38:3057–61.
21. Agarwal G, Reddy GB. Study of surface morphology and optical properties of Nb_2O_5 thin films with annealing. J Mater Sci-Mater El. 2005;16:21–4.
22. Peiffert C, Nguyen-Trung C, Palmer DA, Laval JP, Giffaut E. Solubility of B-Nb_2O_5 and the hydrolysis of niobium(V) in aqueous solution as a function of temperature and ionic strength. J Solution Chem. 2010;39:197–218.
23. Korzhinskaya VS, Kotova NP, Shapovalov YB. Experimental study of natural pyrochlore and niobium oxide solubility in Alkaline hydrothermal solutions. Dokl Earth Sci. 2017;475:793–6.
24. Milozic N, Lubej M, Novak U, Znidarsic-Plazl P, Plazr I. Evaluation of diffusion coefficient determination using a microfluidic device. Chem Biochem Eng Q. 2014;28:215–23.
25. Chen ZG, Li FY, Huang CH. Organic D-π-A dyes for dye-sensitized solar cell. Curr Org Chem. 2007;11:1241–58.
26. Deblonde GJP, Chagnes A, Belair S, Cote G. Solubility of niobium(V) and tantalum(V) under mild alkaline conditions. Hydrometallurgy. 2015;156:99–106.
27. Timofeev A, Migdisov AA, Williams-Jones AE. An experimental study of the solubility and speciation of tantalum in fluoride-bearing aqueous solutions at elevated temperature. Geochim Cosmochim Ac. 2017;197:294–304.
28. Filella M, May PM. The aqueous solution thermodynamics of niobium under conditions of environmental and biological interest. Appl Geochem. 2020;122:104729.
29. Butler C, Cid E, Billet AM. Modelling of mass transfer in Taylor flow: investigation with the PLIF-I technique. Chem Eng Res Des. 2016;115:292–302.
30. Batista LMB, dos Santos AJ, da Silva DR, Alves APD, Garcia-Segura S, Martinez-Huitle CA. Solar photocatalytic application of NbO_2OH as alternative photocatalyst for water treatment. Sci Total Environ. 2017;596:79–86.

31. Natarajan S, Bajaj HC, Tayade RJ. Recent advances based on the synergetic effect of adsorption for removal of dyes from waste water using photocatalytic process. J Environ Sci-China. 2018;65:201–22.
32. Wang Q, Zhang MA, Chen CC, Ma WH, Zhao JC. Photocatalytic aerobic oxidation of alcohols on TiO_2: the acceleration effect of a bronsted acid. Angew Chem Int Edit. 2010;49:7976–9.
33. Mounteer AH, Leite TA, Lopes AC, Medeiros RC. Removing textile mill effluent recalcitrant COD and toxicity using the H_2O_2/UV system. Water Sci Technol. 2009;60:1895–902.
34. Kang YW, Cho MJ, Hwang KY. Correction of hydrogen peroxide interference on standard chemical oxygen demand test. Water Res. 1999;33:1247–51.
35. Yahiaoui I, Aissani-Benissad F, Fourcade F, Amrane A. Enhancement of the biodegradability of a mixture of dyes (methylene blue and basic yellow 28) using the electrochemical process on a glassy carbon electrode. Desalin Water Treat. 2016;57:12316–23.
36. Sapawe N, Jalil AA, Triwahyono S, Adam SH, Jaafar NF, Satar MAH. Isomorphous substitution of Zr in the framework of aluminosilicate HY by an electrochemical method: evaluation by methylene blue decolorization. Appl Catal B-Environ. 2012;125:311–23.
37. Khairnar SD, Patil MR, Shrivastava VS. Hydrothermally synthesized nanocrystalline Nb_2O_5 and its visible-light photocatalytic activity for the degradation of congo red and methylene blue. Iran J Catal. 2018;8:143–50.
38. Patel H, Vashi RT. Characterization and treatment of textile wastewater. Waltham: Elsevier; 2015.

Publisher's Note

Springer Nature remains neutral with regard to jurisdictional claims in published maps and institutional affiliations.

Ready to submit your research? Choose BMC and benefit from:

- fast, convenient online submission
- thorough peer review by experienced researchers in your field
- rapid publication on acceptance
- support for research data, including large and complex data types
- gold Open Access which fosters wider collaboration and increased citations
- maximum visibility for your research: over 100M website views per year

At BMC, research is always in progress.

Learn more biomedcentral.com/submissions

BMC